International Immunopharmacology 70 (2019) 486–497

Contents lists available at ScienceDirect

International Immunopharmacology

journal homepage: www.elsevier.com/locate/intimp

Tanshinone IIA harmonizes the crosstalk of autophagy and polarization in macrophages via miR-375/KLF4 pathway to attenuate atherosclerosis

Wenna Chen[a,b,*], Ximing Li[b], Shengnan Guo[a], Nan Song[b], Junyan Wang[c], Lianqun Jia[b], Aisong Zhu[d]

[a] Department of Medical Science of Laboratory, Liaoning University of Traditional Chinese Medicine, Shenyang, Liaoning, China
[b] Key Laboratory of Ministry of Education for TCM Viscera-State Theory and Applications, Liaoning University of Traditional Chinese Medicine, Shenyang, Liaoning, China
[c] The First Medical College, Guangzhou University of Chinese Medicine, Guangzhou, Guangdong, China
[d] School of Basic Medical Sciences, Zhejiang Chinese Medical University

ARTICLE INFO

Keywords:
Tanshinone
Atherosclerosis
Macrophage
Autophagy
Differentiation

ABSTRACT

Macrophages play a pivotal role in destabilizing atherosclerotic plaque. The diverse phenotypes and complex autophagy in macrophage are observed in atherosclerotic lesions. Tanshinone IIA (TNA) is known as the major component extracted from the root of Chinese herb Salvia miltiorrhiza, used for treatment of cardiovascular diseases. However, the therapeutic mechanism of TNA is not clear yet. In this study, we identified inflammation-related gene expression by microarray in atherosclerotic plaques in ApoE knockout mice fed with high fat diet and found miR-375 was one of the significantly high expressed microRNAs compared with wild type mice and TNA treated mice. Then we compared the levels of proteins related to the signal pathway of autophagy, and the phenotype of macrophages in atherosclerotic plaques ex vivo. We predicted KLF4 might be the key target of miR-375 that mediated the crosstalk between autophagy and polarization by TNA. Furthermore, we detected the expression of signal pathway in ox-LDL induced macrophages after treatment with TNA in vitro to verify this predict. The results suggest TNA could activate KLF4 and enhance autophagy as well as M2 polarization of macrophages by inhibiting miR-375 to Attenuate Atherosclerosis.

1. Introduction

Macrophages are omnipotent immune cells with a plasticity reacted to micro-environmental signals. M1 and M2 are opposite phenotypes of macrophage. Macrophages can be induced classically to M1 phenotype by being exposed to LPS and/or IFN-γ, which are characterized by releasing pro-inflammatory cytokines (such as TNFα and IL-6), iNOS and reactive oxygen species (ROS), and play a crucial role in inflammation initiation and pathogens clearance [1,2]. By comparison, when being exposed to IL-4 or IL-13, macrophages can be activated alternatively and induced to M2 phenotype, which produce anti-inflammatory cytokines (such as IL-10), Arginase-1 and participate phagocytosing apoptotic or dead cells, reducing inflammation, healing wound and repairing tissue [3,4].

Macrophages are essential constituents of atherosclerotic plaques, which play a pivotal role in the process of destabilization. The complexity of macrophage phenotypes was seen in human plaques and atherosclerotic lesions found in atherosclerotic mouse models. Plaque macrophages display a series of phenotypes that exist between M1 (pro-inflammatory) and M2 (anti-inflammatory). Kadl et al. [5] described a new subset of macrophages in advanced plaque called 'Mox'. These cells were stimulated by oxidized phospholipids and exhibited strong anti-oxidant response. Gleissner et al. reported another new subset of macrophage, 'M4' macrophages [6]. These cells were differentiated by CXCL4, carried a lower expression of scavenger receptors (SR) and high levels of cholesterol efflux transporters, which differed from the classically M1/M2 macrophages.

A decade ago, studies on macrophages derived from atherosclerotic

Abbreviations: ox-LDL, oxidized low-density lipoprotein; KLF4, Krueppel-like factor 4; MCP-1, Monocyte chemoattractant protein-1; LPS, lipopolysaccharide; IFN-γ, interferon-γ; CXCL, chemokine (C-X-C motif) ligand; iNOS, inducible nitric oxide synthase; MDC, monodansylcadaverine; TFEB, transcription factor EB; ROS, reactive oxygen species; TNF-α, tumor necrosis factor-α; IL, interleukin; CCR, (C-C motif chemokine receptor); MCPIP, monocyte chemotactic protein-induced protein; NF-κB, nuclear factor kappa-light-chain-enhancer of activated B cells; STAT, Signal transducer and activator of transcription; TNA, Tanshinone II A

* Corresponding author at: Department of Medical Science of Laboratory, Liaoning University of Traditional Chinese Medicine, No. 79, Chongshan Eastern Road, Shenyang, Liaoning, China.
E-mail address: chenwn@lnutcm.edu.cn (W. Chen).

https://doi.org/10.1016/j.intimp.2019.02.054
Received 10 December 2018; Received in revised form 16 February 2019; Accepted 28 February 2019
Available online 12 March 2019

plaques were often limited to the phenotype of macrophages and their role in inflammation. In fact, it has been demonstrated the phenotype of macrophages can adapt to micro-environmental conditions rapidly. In the conditions, the levels of lipids, lipoproteins in serum and the varieties of stimuli by cytokines, chemokines and small bioactive molecules can induce phenotype of macrophage to change into pro-inflammatory or anti-inflammatory properties [7]. Besides the former mentioned subsets, other unidentified populations of macrophage co-exist in plaque probably. Therefore, to reveal the plasticity of macrophage and analyze the functional characteristics of distinct macrophages can help to formulate new strategies for the treatment of atherosclerosis and other chronic inflammatory diseases.

Autophagy is a renovating process, which acts as a key role in keeping intracellular catabolic pathway that maintains intracellular homeostasis. Recently, many evidences in atherosclerosis indicate that there are a series of factors can stimulate autophagy such as ox-LDL [8], metabolic or hypoxia stress [9], endoplasmic reticulum stress [10], reactive oxygen species (ROS) [11], and certain pro-inflammatory cytokines [12]. Razani, et al. indicated that monocyte/macrophages were the predominant cell type that could express autophagy markers in the plaque [13]. Recent research described a specific induction of autophagy in lipid-loaded macrophages that delivered LD to the lysosome and showed the autophagy of the lipid droplet that promoted cholesterol efflux from foam cells [14]. Research suggested the autophagy could promote LDs (lipid droplets) breakdown to liberate FFA (free fatty acids) and cholesterol, which stoke oxidative metabolism and cholesterol efflux, respectively. In addition, macrophage autophagy could limit inflammasome-induced IL-1β production promoted by cholesterol crystals, while defective autophagy was associated with increased IL-1β production [15]. It suggested autophagy could improve efflux of cholesterol and reverse transporting, promote polarization of macrophage into M2 phenotype. Therefore, we believed that there were necessary interrelation between polarized phenotype and autophagy signal of macrophages. However further studies are needed to explore the exact correlation between macrophage autophagy and polarization.

Recently scientists reported herbal medicines acted an important role in improving cardiovascular diseases (CVDs) as anticoagulant [16]. Danshen (*Salvia miltiorrhiza*) has been widely used in traditional folk medicine in China, the United States and several European countries to treat CVDs and cerebrovascular diseases [17]. Researchers reported the effects of Danshen on CVDs and the novel underlying mechanism of its main constituents on improving the function of platelets and hemostasis [18]. Tanshinone IIA (TNA) is the main fat-soluble monomer component, which is extracted from the root of Danshen. In recent days, TNA exhibits various pharmacological properties, such as antioxidant, anti-apoptosis and anti-inflammatory activities [19–21] and has been identified in clinic as anti- atherosclerosis drug [22]. However, the mechanism of TNA in the treatment of atherosclerotic diseases is not clear yet.

MicroRNAs is the key regulators of metabolic homoeostasis, which found a decade ago. Amount of circulating miRNAs are detected in serum emphasizes their important role as both endocrine regulator and possible markers of disease. MiRNAs dysregulation in metabolic diseases, such as obesity, diabetes and atherosclerosis implies their potential as therapeutic targets. We detected the microRNA expression in aortas by microarray in previous study and found many microRNAs differ in ApoE knockout mice from wild type mice. Especially, miR-375 was significantly upregulated in ApoE$^{-/-}$ mice. At present, most research are focus on the biology function in cancer cells and its exact effect on the metabolic disease is undefined Research shows increased miR-375 levels has been implicated in rodent models of myocardial infarction and the patients with heart failure [23]. Studies provide evidence that miR-375 could regulate Kupffer cells to improve immune function in mice with liver failure [24]. Then we predicted the targets of miR-375 with the computer-aided algorithms and found one of the targets–KLF4 participated in the activation of both autophagy and polarization signaling pathways. Therefore, we hypothesize that KLF4 may be a main target of miR-375 to mediate the crosstalk of autophagy and polarization in atherosclerotic plaques. In the study, we try to reveal the mechanism of TNA mediating the crosstalk between polarization and autophagy of macrophages in the role of anti-atherosclerosis.

2. Materials and methods

2.1. Mice experiments

All mice were bought from Beijing Vital River Experimental Animal Technology Co, Ltd. (Beijing, China). Mice were divided into three groups: control group, model group and TNA group (10 mice for each group). Mice in model group and TNA group were Apolipoprotein E–deficient (ApoE$^{-/-}$) C57BL/6J mice (male, 4-6 week age) fed for 20 weeks with high-fat diet of 21% butter fat and 0.15% cholesterol (Specialty Feeds) commencing at 8 weeks of age. ApoE$^{-/-}$ mice in TNA group were treated with 10 mg/kg TNA (> 98.0% pure, Sigma-Aldrich, USA) by intraperitoneal injection once a day at the same time. Mice in control group were wildtype with C57BL/6J background (male, 4-6 week age) fed with normal diet.

Then the mice were anaesthetized with 5% isoflurane, and the blood was collected by cardiac puncture, and aortic sinus and arch were collected for histology and molecular studies, respectively. In accordance with the NIH Guide (NIH Publications No. 8023, revised 1978), the study was conducted for the Care and Use of Laboratory Animals. All protocols were approved by the Animal Ethics Committee of Liaoning University of Traditional Chinese Medicine.

2.2. Plasma cholesterol and triglycerides

Plasma cholesterol and triglycerides were determined enzymatically using a Beckman CX7 chemistry autoanalyzer (Beckman Coulter Diagnostics, Fullerton, CA). Plasma triglycerides were measured with Infinity™ Triglycerides kit (Thermo Scientific). HDL and LDL cholesterol were determined using homogeneous assay kits (Equal Diagnostics, Exton, PA).

2.3. Histological analysis

The proximal aorta of mice was dissected and embedded in OCT compound and 4 μm slices were cut and then frozen in −80 °C for staining. For H&E (hematoxylin–eosin) staining, slices were stained with hematoxylin (Gill's formula H-3401, Vector Laboratories) for 3 min, washed and treated with acid ethanol. Then slices were incubated with 2% eosin for 3 min and washed again. The average size of plaque within the aortic intima for each slice was calculated by measurement of cross sections in the ascending aorta [25,26]. For Oil-Red O staining, slices were fixed with formalin, and then rinsed with 60% isopropanol. Next, slices were stained with freshly prepared Oil Red O working solution for 15 mins. Lastly, nuclei were stained with alum hematoxylin after rinse with 60% isopropanol. Then the average size of lipid accumulation within the aortic intima for each slice was quantified by the percentage of Oil-Red O positively stained area using Image Pro (Silver Springs, MD).

2.4. Isolating aortic macrophages by cell sorting

The aortas were dissected into small pieces and incubated in HEPES-enzyme cocktail for 1 h with gentle shaking as described in previous study [27]. Then the digesta were filtered by 70-μm cell strainer (Falcon), and the cell were treated with red blood cell lysis buffer (Biolegend, San Diego, CA). Next, the cells were centrifuged and resuspended in 5% FBS/PBS. Half of the cells were performed for immunofluorescent staining. The other cells were incubated with anti-CD11b -APC, anti-F4/80-PECy7 (Biolegend, San Diego, CA) and

analyzed by a BD Aria flow cytometer (Becton Dickinson, San Jose, CA). The average percentage of $F4/80^+$ $CD11b^+$ cells (macrophages) was approximately 35 ± 10%. The primary macrophages were sorted (purity > 90%) for the RT-qPCR or WB assay.

2.5. Immunofluorescent staining of LC3B and macrophages phenotype

The aortic macrophages were incubated on coverslips in 24well plate for 1 h at 37 °C. Unattached cells were washed out with 5% FBS/PBS and adherent cells (macrophages > 75%) incubated with primary antibodies for anti-rat-anti-CD206-FITC and rat-anti- CD197-PE after blocked with 10% normal goat serum. Then cells were fixed with 4% paraformaldehyde, permeabilized and stained with rabbit-anti-LC3B for 1 h. Next, secondary antibodies, goat anti-rabbit-Dylight 405 was added continuously for 1 h. Fluorescence microscope (Olympus BX51) was used to image the fluorescent staining. All fluorescent images are at a 400× final magnification. Three fields (about 15–20 cells/field) images were randomly obtained to determine fluorescent expression per sample.

2.6. Staining Isolated aortic macrophages by Oil Red O

The aortic macrophages were incubated on coverslips in 24well plate for 1 h at 37 °C. Unattached cells were washed out with 5% FBS/PBS and then adherent cells were stained with Oil Red O as follows. Cells were fixed in 10% (v/v) formalin (Sigma-Aldrich) for 1 h and washed with 60% (v/v) isopropanol. The cells were then stained with Oil Red O for 10 min. Nuclei were stained with alum hematoxylin after rinse with 60% isopropanol and then cells were observed by light microscopy.

2.7. Analysis of gene expression by RT-qPCR

Total RNA was isolated from cells collected from three groups using Trizol reagent (Invitrogen). Then total RNA was used for qRT-PCR using Biotool™ SYBR Green qPCR Master kit (Selleckchem, Houston, TX, USA) following the manufacturer's instructions. The relative gene expression of M1 associated markers (TNF-a, IL-6, iNOS and IL-12), M2 associated markers (Arg-1, IL-10 and MCPIP), were quantified with β-actin as a reference control. The primers were listed in Table 1. The $2^{-\Delta\Delta Ct}$ method was used to analyze the results of the qRT-PCR.

Table 1
Sequences of primers used for RT-qPCR.

Gene	Sequences of primers	NCBI reference sequence
β-Actin	F 5′-CATCCGTAAAGACCTCTATGCCAAC-3′ R 5′-ATGGAGCCACCGATCCACA-3′	NM_007393.5
TNF-α	F 5′-TCTTCTCATTCCTGCTTGTGG-3′ R 5′-GGTCTGGGCCATAGAACTGA-3′	NM_001278601.1
IL-6	F 5′-GGAGCCCACCAAGAACGATAG-3′ R 5′-GTGAAGTAGGGAAGGCCGTG-3′	NM_001314054.1
IL-12	F 5′-AAACCATCCAGGTTCGCCAT-3′ R 5′-AAGGAGTGTGGCCATTGTGT-3′	NM_ 001303244.1
iNOS	F 5′-CCCTTCAATGGTTGGTACATGG-3′ R 5′-ACATTGATCTCCGTGACAGCC-3′	NM_001313922.1
Arg-1	F 5′-AGACAGCAGAGGAGGTGAAGAGTAC-3′ R 5′-GGTAGTCAGTCCCTGGCTTATGGT-3′	NM_007482.3
IL-10	F 5′-CAGAGCCACATGCTCCTAGA-3′ R 5′-TGTCCAGCTGGTCCTTTGTT-3′	NM_010548.2
MCPIP	F 5′-TGAGCCATGGGAAGAAGGAAGTCT 3′ R 5′-TGTGCTGGTCTGTGATAGGCACAT 3′	NM_153159.2
KLF4	F 5′-CGGGAAGGGAGAAGACACT R 5′-GAGTTCCTCACGCCAACG	NM_010637.3

F, forward; R, reverse.

2.8. Analysis of gene and microRNA expression by microarray

Total RNA was isolated from aortas according to suppliers' instructions. The procedure began with the conversion of experimental RNA samples into first-strand cDNA using the RT2 First Strand Kit. Next, the cDNA was mixed with an appropriate RT2 SYBR Green Mastermix. This mixture was aliquoted into the wells of the RT2 Profiler PCR Array (PAMM-077Z, QIAGEN Inc., Valencia CA, USA). For microRNA assay, excluding the Custom RT Primer Pool, all additional reagents necessary for the multiplex RT step were contained in the TaqMan® MicroRNA Reverse Transcription Kit (No. 4366596). Loaded and run the array using Custom TaqMan® Array MicroRNA Card (No. 4371129) default thermal-cycling conditions. For analysis of Comparative CT (RQ), refer to the Applied Biosystems® 7900 HT Fast Real-Time PCR System Relative Quantitation Using Comparative CT Getting Started Guide (No. 4364016). The expression level of mature miRNAs was calculated using U6 as an internal control. Each sample was tested in triplicate.

2.9. In-vitro culture of Raw264.7 cells

Murine RAW264.7 cells were cultured in 25 cm flasks in RPMI 1640 with 10% FBS and 0.05 mM β-mercaptoethanol. Next, the cells were randomly divided into control group, ox-LDL group, TAN group and ox-LDL + TAN group. Cells in ox-LDL group were treated with ox-LDL 50 μg/ml for 8 to 24 h. Cells in TAN group were treated with TNA (10 μg/μl). Cells in ox-LDL + TAN group were treated with 50 μg/ml ox-LDL and TNA (10 μg/μl). Cells in control group were cultured without treatment. To reveal the effect of TNA on autophagy, the autophagy vacuoles in RAW264.7 cells treated with ox-LDL (50 μg/ml) were analyzed for 8, 16 and 24 h separately with or without TNA.

2.10. Qualified of autophagic vacuoles by monodansylcadaverine (MDC) staining

The RAW264.7 cells were incubated on coverslips in 24well plate for 1 h at 37 °C, and then were treated with ox-LDL or TNA for 8 to 24 h as described above. Then autophagic vacuoles were labeled with 0.05 mM MDC in PBS at 37 °C for 10 min [28]. After incubation, cells were washed with PBS and immediately analyzed using fluorescence microscopy (Nikon Eclipse TE2000, Tokyo, Japan) with 380–420 nm excitation filter and 450 nm barrier filter. Images were obtained with a CCD camera and analyzed by Meta View 4.5.

2.11. Transient transfection with miR-375 mimics

RAW264.7 cells were cultured in 6-well cell culture plates to ~70% confluence. Cells were transfected with either 10 pmol miR-375 mimics as the transfection reagent (GenePharma Inc., Shanghai, China) according to the manufacturer's instructions. The sequence of miR-375 mimics: 5′-ACUGGACUUGGAGUCAGAAGG-3′, 5′-UUCUGACUCCAAG UCCAGUUU-3′; The sequence of miR-375 inhibitor: 5′-CCUUCUGACU CCAAGUCCAGU-3′. After gene transfection for 6 h, the medium was changed and the cells were cultured until 48 h. Then cells were treated by 50μg/ml ox-LDL with or without TNA for 24 h and collected for qPCR or western blot analysis. The supernatants were collected from each well for ELISA assay.

2.12. ELISA assay

The cytokine secretion in supernatant by M1 cells (TNF-a, IL-6, iNOS and IL-12) and M2 cells (Arg-1, IL-10 and MCPIP), was detected by ELISA kits (Bio-rad, USA) according to the instructions. The absorbance was measured using a microplate reader at 490 nm.

2.13. Western blot analysis

Western blot was performed as previously reported [2]. In brief, cells were lysed on ice for 30 min in RIPA buffer (pH 7.4 50 mM Tris, 150 mM NaCl, 1% NP-40, 0.5% sodium deoxycholate, 0.1% SDS) supplemented with 1 mM PMSF, protease inhibitor cocktail, sodium orthovanadate and sodium fluoride. The lysates were resolved by SDS-PAGE and transferred to nitrocellulose and cultured with appropriate primary antibody (MCPIP, KLF4, STAT6, pSTAT6, NFκb, NFκb p65, LC3, Beclin1, GAPDH) and HRP labeled secondary antibody (all from Cell Signaling Technology Inc., Danvers, MA, USA), and proteins were visualized using an ECL kit (Pierce, Rockford, CA, USA) and then exposed with a Visualizer. The intensity of bands was quantified with Image J software by densitometry.

2.14. 3′ UTR-luciferase reporter constructs

The wild-type or mutant 3′ UTRs of KLF4 containing the predicted miR-375 binding sites were synthesized (Gene Art, Life technologies, Germany) and cloned into the pGL3.0-control vectors according to the manufacturer's instructions (Promega, Madison, WI). RAW264.7 cells were transfected with 10 pmol miR-375 mimics or scramble controls (Qiagen) and co-transfected with 0.2 mg per well wild-type KLF4 3' UTR-luc or mutant 3' UTR-luc, respectively using JetPEI transfection reagent (Polyplus transfection, Illkirch, France) according to the manufacturer's instructions. pRL-TK vectors (0.01 mg per well) were co-transfected as endogenous controls for luciferase activity. After 24 h of transfection, lysis was performed and luciferase activity was detected by a dual-luciferase assay kit (Promega).

2.15. Statistical analysis

Statistical analyses of experiments involving only two groups were performed using a two-tailed Student' *t*-test. For multiple comparisons, the p value was determined by Two-way ANOVA followed by a Bonferroni posttest. All analyses were performed with GraphPad Prism 5 software. A value of $p < 0.05$ was statistically significant. Data are shown as mean ± SD.

3. Results

3.1. The levels of Plasma cholesterol and triglycerides

The plasma triglycerides (TG), total cholesterol (CHO), HDL and LDL cholesterol were measured in ApoE$^{-/-}$ mice or wildtype mice. The results showed that the levels of TG, CHO, LDL in the plasma of mice in model group were increased and obviously higher levels in comparison with control group ($p < 0.01$), while the levels of HDL were lower, but the difference was not significant ($p > 0.05$). Compared with mice in model group, the levels of TG ($p < 0.01$) CHO ($p < 0.05$) and LDL ($p < 0.05$) were lower in mice of TAN group, while the levels of HDL were higher ($p < 0.05$), Fig. 1A. The results suggested that TAN could downregulate TG, CHO and LDL and upregulated HDL effectively.

3.2. Quantification of atherosclerotic lesions

To detect the atherosclerotic lesions, atherosclerotic plaque in the aortic root of mice in three groups were assessed via intimal lesion areas and lipid accumulation in photomicrographs. The intimal lesion areas with H&E staining were obviously larger in model group and TAN group than that in control group ($p < 0.01$), and it was nearly double in model group in comparison with TAN group ($p < 0.01$). The lipid accumulation with Oil Red O staining was obvious in model group and TAN group in comparison with control group ($p < 0.01$), and decreased in TAN group compared with model group ($p < 0.01$), shown in Fig. 1B, C. The results suggested that TAN could attenuate lipid accumulation in aorta and improve the restore of atherosclerotic lesions.

3.3. Immunofluorescence analysis of LC3b and phenotype of macrophages from the atherosclerotic lesions macrophages

To clarify the phenotype of macrophages in the atherosclerotic plaques, we analyzed the number of LC3 puncta and phenotypic markers on macrophages in aorta by immunofluorescence staining. The autophagosome formation and macrophage phenotypes were quantified (Fig. 2A, B). Quantitative analysis revealed that the expression of CD197 was significantly enhanced in the model group ($p < 0.05$) compared with the WT mice. CD197 expression was significantly inhibited in the TAN group ($p < 0.05$) compared with the model group, while the expression of CD206 in the TAN group was significantly enhanced ($p < 0.01$). For autophagosome formation, it showed that CD206^{+} macrophages expressed higher LC3 puncta than CD197 $^{+}$ macrophages ($p < 0.01$). It suggested that M2 phenotype has higher expression of autophagosome. In addition, compared with the model group, macrophages expressed higher LC3 puncta in TAN group ($p < 0.01$), shown in Fig. 2C. To observe the overall status of autophagy in the aortal tissue, the relative expression of LC3b was detected by western blot. The result showed the relative expression of LC3b was significantly enhanced in the model group and TAN group ($p < 0.01$) compared with the WT mice and it was especially higher in the TAN group ($p < 0.01$) compared with the model group, shown in Fig. 2E. These results showed that the accumulation of macrophages in the atherosclerotic lesions of the aortic root of model mice were mainly M1 phenotype (with high lipid accumulation and the low levels of autophagosome formation), and M2 polarization of macrophages became the predominant subset in TAN group (with less lipid accumulation and high levels of autophagosome formation).

3.4. The lipid accumulation in macrophages from atherosclerotic lesions by Oil Red O staining

To observe the lipid accumulation in aorta macrophages stained with Oil Red O, we qualified the percentage of positive cells in aorta macrophages. It was obvious in model group vs. control group ($p < 0.01$), and decreased in TAN group compared with model group ($p < 0.01$), shown in Fig. 2D. The results suggested that TAN could attenuate lipid accumulation in aorta.

3.5. Analysis of autophagy vacuoles in RAW264.7 cells by fluorescence microscopy

Since the macrophages from atherosclerotic lesions cannot been cultured in vitro for long time, we cultured RAW264.7 cells in vitro instead of them intend to reveal the in-depth mechanism of macrophages polarization and autophagy induced by TAN. Cells treated with ox-LDL (50 μg/ml) were analyzed for 8, 16 and 24 h separately with or without TNA. To further assess the putative role of autophagy induced by ox-LDL with or without TNA, these cells were stained with MDC and observed under fluorescence microscopy. The autophagosome formation was qualified by software.

The results showed that autophagy vacuoles were accumulated after ox-LDL treated for 16-24 h, compared with control cells ($p < 0.01$), but no obvious difference was found in only TNA treated cells ($p > 0.05$ vs. control). In contrast, it showed an obvious increase in the number of vesicles as well as in their size in TAN + ox-LDL treated cells ($p < 0.01$ vs. ox-LDL group), shown in Fig. 3A, B. This result indicated that TNA induced the formation of the MDC-labeled vacuoles 16 h to 24 h after ox-LDL treated, especially 24 h. Therefore, we selected 24 h as the time point in followed tests.

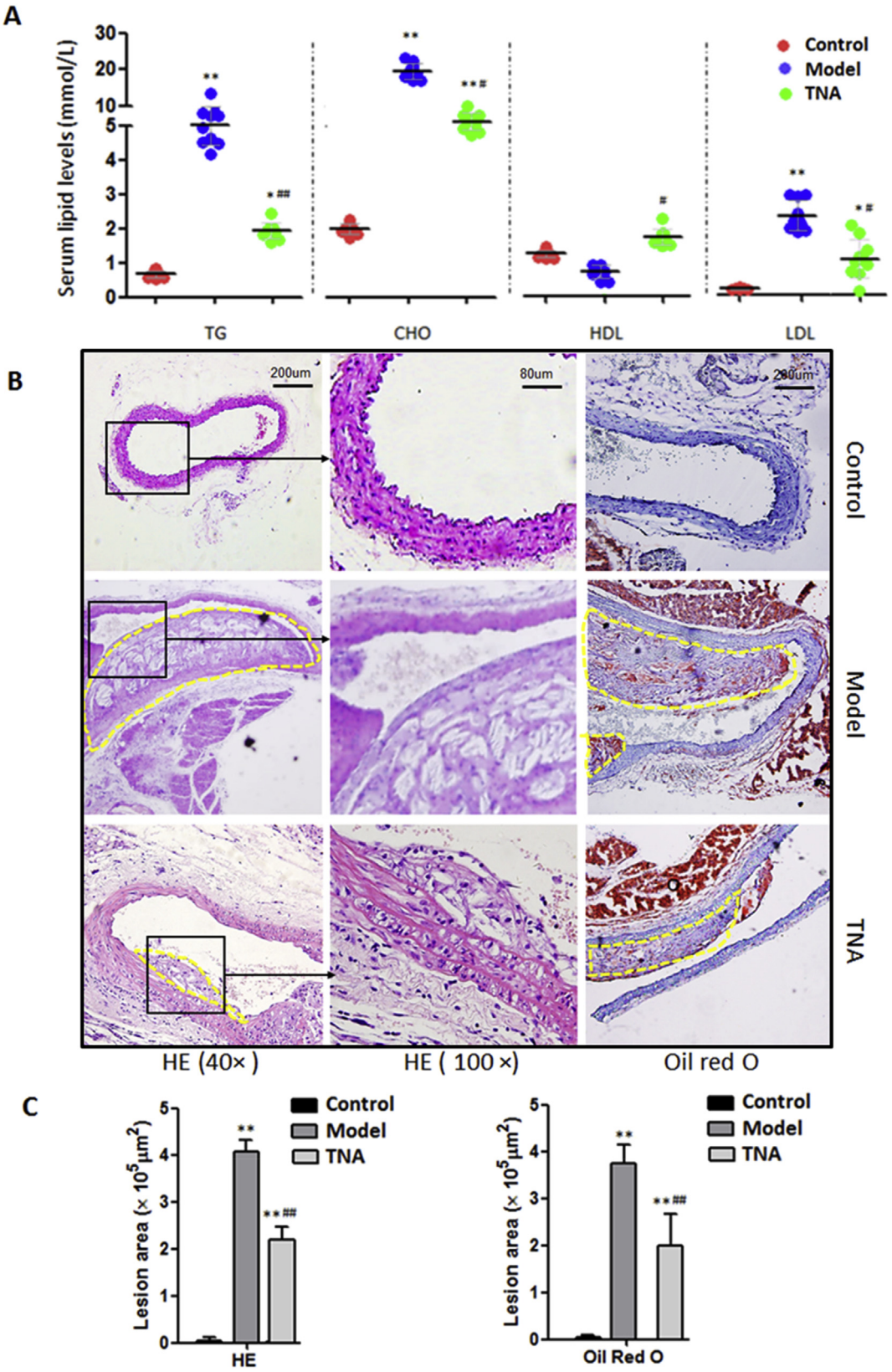

Fig. 1. Plasma lipid levels and atherosclerotic lesions in the aorta of ApoE $^{-/-}$ mice or WT mice.
ApoE $^{-/-}$ Mice were fed on high fat diet for 20 wk with or without TNA. A, Plasma triglycerides (TG), the levels of total cholesterol (CHO), HDL and LDL cholesterol in plasma were measured in ApoE $^{-/-}$ mice or WT mice; Data present mean ± SD. n = 8 to 10 per group. *p < 0.05 and **p < 0.01 vs. control group; $^{\#}$p < 0.05 and $^{\#\#}$p < 0.01 vs. model group. B, H & E and Oil Red O staining of representative aortic slices. The atherosclerotic intimal lesions were circled in yellow lines. Bar represents 200 μm or 80 μm; C. Bar graphs represent intimal lesion areas (H&E) and lipid accumulation (Oil Red O). Data present mean ± SD. n = 5 per group. **p < 0.01 vs. control group; $^{\#\#}$p < 0.01 vs. model group. (For interpretation of the references to color in this figure legend, the reader is referred to the web version of this article.)

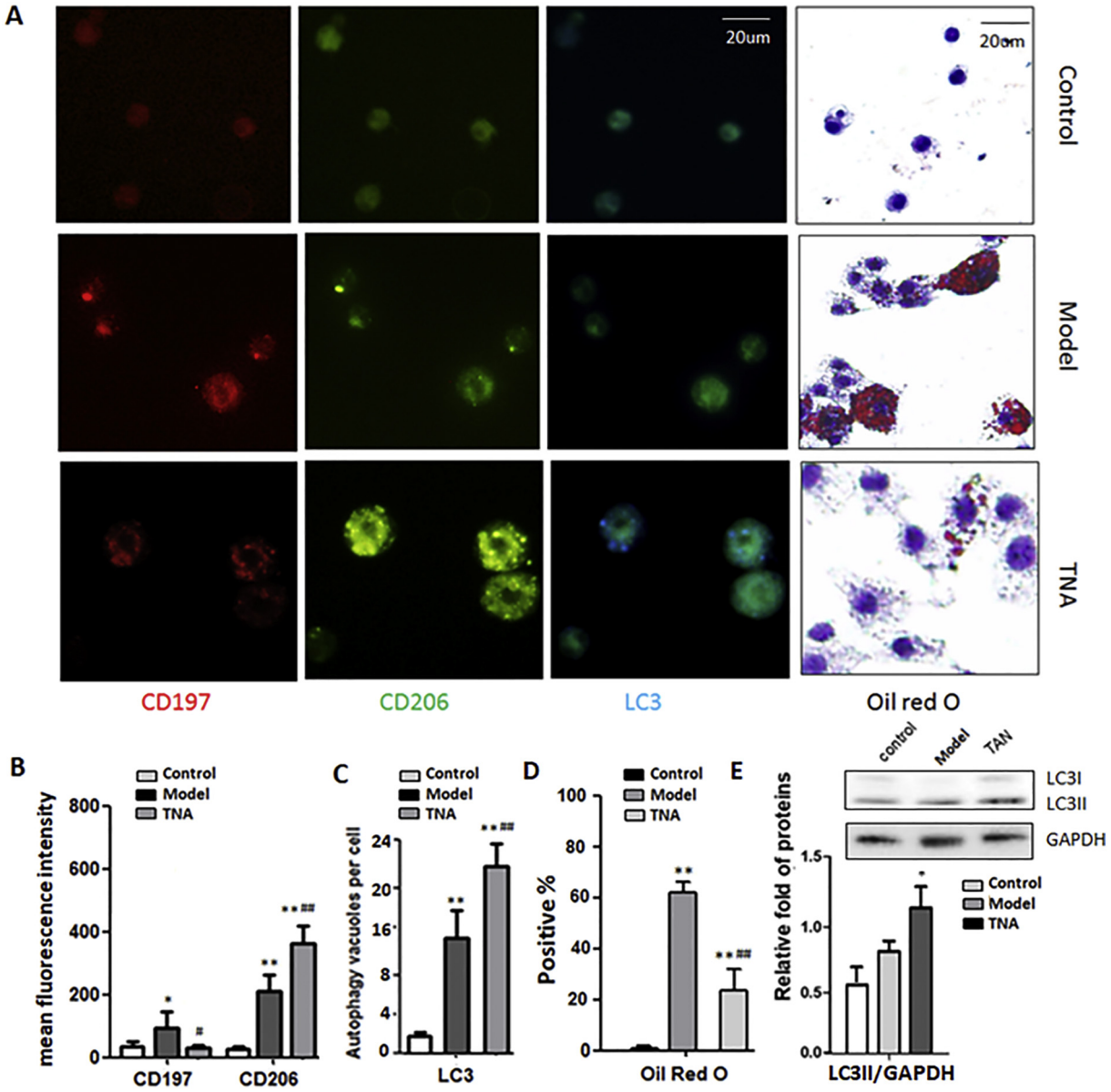

Fig. 2. LC3 puncta quantification and phenotype markers on aortic macrophages from ApoE$^{-/-}$ mice with/without TNA or WT mice.
A. The slices of aortas were stained with antibodies against LC3, CD197 and CD206. Representative photomicrographs demonstrated CD206 positive cells (M2) in green, CD197 positive cells (M1) in red, LC3 positive cells in blue. Right column showed the lipid accumulation in macrophages by Oil Red O staining. Scale bar = 20 μm. B. The analysis of phenotype of aortic macrophages. The histogram shows quantitative analysis of the mean fluorescence intensity of CD197 and CD206. Data present mean ± SD. n = 3 per group. *p < 0.05 and **p < 0.01 vs. control group; $^{\#}$p < 0.05 and $^{\#\#}$p < 0.01 vs. model group. C. The analysis of LC3 puncta quantification of aortic macrophages. The histogram shows quantitative analysis of the autophagy vacuoles per cell. Data present mean ± SD. n = 3 per group. **p < 0.01 vs. control group; $^{\#\#}$p < 0.01 vs. model group. D. The percentage of positive cells of aortic macrophages stained with oil red O. Data present mean ± SD. n = 3 per group. **p < 0.01 vs. control group; $^{\#\#}$p < 0.01 vs. model group. E. the relative expression of LC3II in aortic macrophages by WB assays. (For interpretation of the references to color in this figure legend, the reader is referred to the web version of this article.)

3.6. Analysis of gene expression in cultured RAW264.7 by RT-qPCR

RT-qPCR was performed for genes of cytokines (TNF-a, IL-6, IL-12, IL-10, iNOS, Arg-1 and MCPIP) in cells treated with ox-LDL with/without TNA for 24 h. As shown in Fig. 3C, there was a significant increase of the pro-inflammatory cytokine (TNF-a, IL-6, iNOS, IL-12) after being treated with ox-LDL, compared with control (p < 0.01 or 0.05), but no obvious difference was found in only TNA treated cells (p > 0.05 vs. control). Whereas a decreased tendency was found after TNA + ox-LDL treated, compared with ox-LDL (p < 0.01 or 0.05).

The expression of the anti-inflammatory cytokine (IL-10, Arg-1 and MCPIP) was observed no obviously changed after being treated with ox-LDL or TNA only, but it showed significantly increased expression after treated with TNA + ox-LDL, compared with control (p < 0.01 or 0.05). It was an interesting find that the levels of MCPIP were upregulated significantly after being treated with TNA + ox-LDL, compared to control group and ox-LDL (Fig. 3C).

Research demonstrated interact of KLF4-MCPIP can mediate the M2 polarization induced by IL-4. At the same time, we detected the mRNA expression of KLF4 and MCPIP in macrophages isolated from aortas of mice. It was shown that the mRNA level of KLF4 and MCPIP in ApoE$^{-/-}$ mice was higher than that in control mice, and the levels of KLF4 and MCPIP were upregulated significantly after being treated with TNA + ox-LDL, compared to ApoE$^{-/-}$ mice (p < 0.05, Fig. 3D).

To validate results of qPCR, we detected the expression of KLF4 and MCPIP at protein level by Western Blot. This is consistent with previous

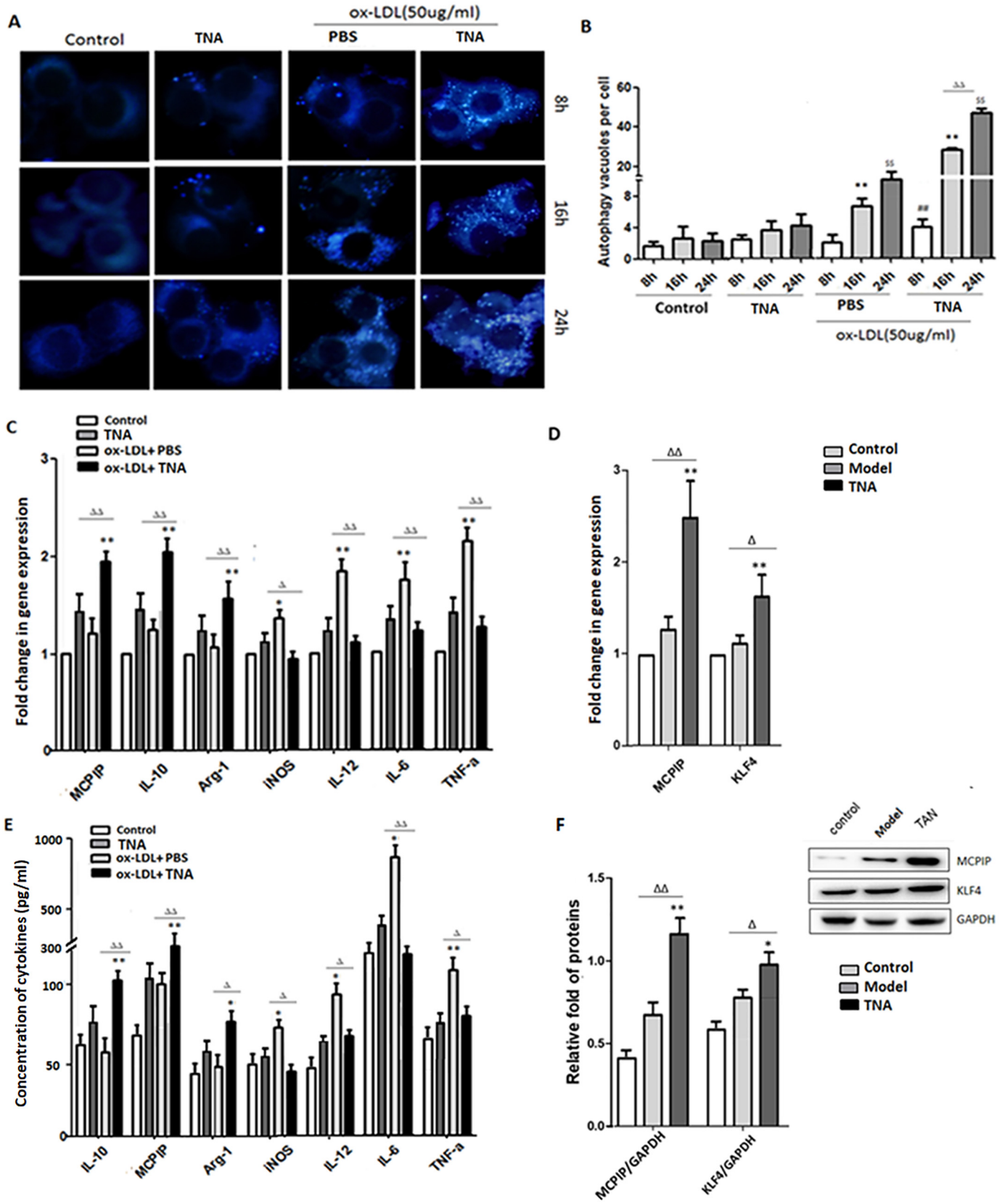

(caption on next page)

results indicating the levels of KLF4 and MCPIP were upregulated significantly after being treated with TNA + ox-LDL shown in Fig. 3F.

Since MCPIPs also possess activity of RNase which can induce autophagy [29], we predict KLF4 might be the key target that mediates the crosstalk between autophagy and polarization of macrophages. So we try to detect the exact function of KLF4 on autophagy and

Fig. 3. Analysis of autophagy vacuoles and expression of cytokines in RAW264.7 cells treated with ox-LDL with/without TNA or macrophages from aorta of mice. A. analysis of autophagy vacuoles in RAW264.7 cells treated with ox-LDL with/without TNA. Cells were stained with monodansylcadaverine (MDC) and analyzed by fluorescence microscopy. B. The histogram indicates that quantification of autophagy vacuoles numbers in RAW264.7 cells. Data present mean ± SD. n = 3 per group. $^{\#\#}p < 0.01$ vs. control 8 h; $^{**}p < 0.01$ vs. control 16 h; $^{\$\$}p < 0.01$ vs. control 24 h. $^{\Delta\Delta}p < 0.01$ vs. indicated group. C. The analysis of mRNA levels in the RAW264.7 cells treated with ox-LDL with/without TNA for 8 h, 16 h and 24 h. The inflammatory-related genes were assayed by RT-qPCR. D. The analysis of mRNA levels in the macrophages from aorta of mice by RT-qPCR. The data were normalized to the expression level of β-actin mRNA and the $2^{-\Delta\Delta Ct}$ method was used to analyze the results; n = 5; Data present mean ± SD. $^{*}p < 0.05$ and $^{**}p < 0.01$ vs. control. $^{\Delta\Delta}p < 0.01$, $^{\Delta}p < 0.05$ vs. indicated group. E. ELISA assay of cytokines secreted by RAW cells. n = 3; Data present mean ± SD. $^{*}p < 0.05$ and $^{**}p < 0.01$ vs. control. $^{\Delta\Delta}p < 0.01$, $^{\Delta}p < 0.05$ vs. indicated group. F. WB assay of protein expression in macrophages from aorta of mice. n = 3; Data present mean ± SD. $^{*}p < 0.05$ and $^{**}p < 0.01$ vs. control. $^{\Delta\Delta}p < 0.01$, $^{\Delta}p < 0.05$ vs. indicated group.

polarization signal pathway in macrophages after ox-LDL treated with/without TNA in the following study.

3.7. The concentration of cytokines secreted by RAW264.7 cells with ELISA assay

For the cytokine secreted by RAW cells, we carry out ELISA assay to validate the results of qPCR. As shown in Fig. 3E, there was a significant increase of the pro-inflammatory cytokine (TNF-a, IL-6, iNOS, IL-12) after being treated with ox-LDL, compared with control ($p < 0.01$ or 0.05), but no obvious difference was found in only TNA treated cells ($p > 0.05$ vs. control). Whereas a decreased tendency was found after TNA + ox-LDL treated, compared with ox-LDL ($p < 0.01$ or 0.05). The expression of the anti-inflammatory cytokine (IL-10, Arg-1 and MCPIP) was observed no obviously changed after being treated with ox-LDL or TNA only, but it showed significantly increased expression after treated with TNA + ox-LDL, compared with control ($p < 0.01$ or 0.05). These results indicated TNA could act the role of anti-inflammation in ox-LDL treated cells.

3.8. The analysis of miRNAs expression by microarray

To determine whether any miRNAs were involved in post-transcriptional modulation of KLF4, we monitored the alterations of miRNAs in aortas. We found that miR-375 was significantly upregulated ($-$Log2 [fold change] > 2) in ApoE$^{-/-}$ group, compared to WT group, but the differentiation is not obvious between TNA group and WT group ($2 >$ Log2 [fold change] > 1), shown in Fig. 4A. We next used a TaqMan probe–based quantitative RT-PCR assay to further validate the expression levels of miRNAs in the microarray data. As shown in Fig. 4B, the level of miR-375 was strongly increased in aorta of ApoE$^{-/-}$ mice compared with WT mice ($p < 0.05$), but the levels were no significant difference between TNA group and WT group ($p > 0.05$). This result suggested TNA could down-regulate the expression of miR-375 responded to high fat diet. However, whether KLF4 gene is the main target of miR-375 is still unclear. Therefore, we tried to predict and confirm the exact relationship between miR-375 and KLF4 in next experiment.

3.9. Bioinformatics analysis and luciferase assay

To predict whether miR-375 could target 3′ UTR of KLF4 and regulate transcript and expression of KLF4, we carried out bioinformatics analysis with the computer-aided algorithms TargetScan, miRanda, RNAhybrid and PITA. As shown in Fig. 4C, we predicted that miR-375 could target the sequence within the 3' UTR of KLF4, and this result suggested that KLF4 might be a common target gene of miR-375. The miR-375 was predicted binding to the position of 776–805 3′ UTR of KLF4. To validated the exact target, luciferase assay was performed to confirm the specific binding of miR-375 to the 3′ UTR of KLF4 (Fig. 4D). So we hypothesize mir-375 might mediate the KLF4 inhibition and further induced the crosstalk of autophagy and polarization of macrophages.

3.10. The expression of protein related to polarization and autophagy signal pathway regulated by TNA

It was known that NF-κB is important transcription factor that regulates the expression of genes relative with M1 phenotype. In contrast, IL-4 and IL-13 promote the M2 phenotype via STAT6 activation [30,31]. It was reported that STAT6 and KLF4 could induce each other and function cooperatively to induce M2 polarization [32]. It was also shown that KLF4 mediated induction of ER stress probably could contribute to the activation of autophagy. To determine the functional role of miR-375/KLF4 in macrophages polarization and autophagy induced by ox-LDL, we detected the expression of protein in the signaling pathway related with autophagy and polarization of RAW cells by western blot. The results showed that the levels of MCPIP was upregulated after being treated with TNA, compared with ox-LDL treated only ($p < 0.05$), and the expression of Beclin1 and LC3 II were increased at the same time ($p < 0.05$). The expression of p-STAT6 was upregulated significantly ($p < 0.05$ vs. control), while the levels of phosphorylation of NF-κB were downregulated obviously after TNA treated, compared with ox-LDL treated ($p < 0.05$ vs. control). MiR-375 inhibitor was shown similar effect with TNA. After treated by TNA with miR-375 mimics, the expression of Beclin1 and LC3 II and phosphorylation of STAT6 was attenuated ($p < 0.01$ vs. TNA group), while the phosphorylation of NF-κB was enhanced compared with control ($p < 0.01$), as shown in Fig. 5A, B. The results revealed that miR-375/KLF4 mediated the effect of TNA of activating autophagy and the induction of M2 polarization in the role of anti-inflammation.

4. Discussion

Atherosclerosis is a chronic inflammatory response with artery-wall thickening, invasion and accumulation of foam cell. Monocytes act a key role in the progression by migrating into the lesions and differentiate into macrophages. As we have known, macrophages can polarize into specific phenotypes, like M1 (classically activated macrophages) or M2 (alternatively activated macrophages) in atherosclerotic plaque. Previous study showed the ratio of M1 to M2 macrophages could determine the severity and progression of lesions. It showed that the stable plaque was mainly composed of M2 macrophages, and the proportion of M1 was increasing in unstable plaque [33]. Macrophages are exposed to complex environmental conditions, such as lipids, inflammatory cytokines et.al, which modulates their functional phenotypes in the progress of atherosclerotic plaque. Therefore, targeting on specific macrophage subsets at different sites or stages of atherosclerotic lesions may be a sound approach in cardiovascular disease.

Previous study suggested that certain infectious agents could induce monocyte to migrate into endothelial and differentiate into macrophages to swallow a large amount of lipid on the early onset of atherosclerosis. Then they changed into foam cells to secrete inflammatory cytokines and adhesion molecules, chemotaxis of lymphocytes, increasing endothelial damage, causing proliferation, migration of smooth muscle cell, and causing the ingredient changes of matrix collagen. The atherosclerotic circumstances could induce macrophages differentiate into M1 cells, and M2 cells could weaken high inflammatory state due to M1 polarization [34,35]. Recent studies reported that the numbers of both M1 and M2 macrophages were

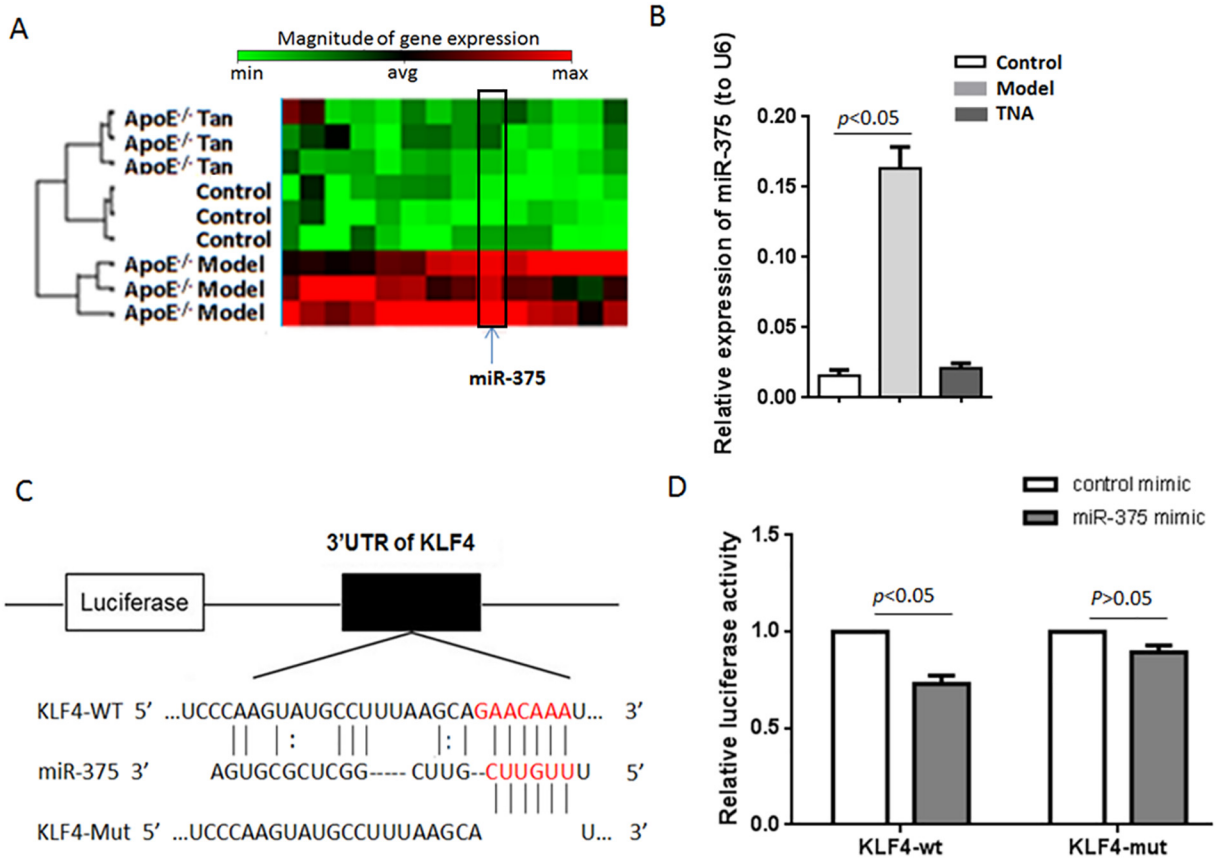

Fig. 4. miRNAs expression by microarray and luciferase assay.
A. The analysis of miRNAs expression in aortas from WT, ApoE$^{-/-}$ and TNA treated mice by microarray. B. The histogram indicates the expression of miR-375 in aortas from WT, ApoE$^{-/-}$ and TNA treated mice by RT-qPCR. Data present mean ± SD. n = 3 per group. C. The predicted target of miR-375 binding to 3′ UTR of KLF4 by bioinformatics. D. Luciferase assay was performed to confirm the specific binding of miR-375 to the 3' UTR of KLF4. Data present mean ± SD. n = 3.

increased during plaque progression, M1 macrophages were the main population in rupture-prone shoulder regions and distributed in progressing plaques; however, M2 macrophages were far from the lipid core of the plaque and primary in unstable plaque [36,37]. Th2 cytokines appear in the patient's plasma with advanced AS, which activates the M2 macrophage to promote the formation of the fibrous cap, and thereby enhance the stability of the plaque [38]. Studies also show that M2 macrophages can repair and remodel the damage tissue in the latter of inflammatory response [39]. Therefore, differentiation of macrophages can not only reduce immune injury to blood vessels by M1 macrophages, but also enhance the anti-inflammatory ability of M2 macrophages and promote blood vessel repair, which may lead to a new clinical strategy for AS treatment.

Autophagy of macrophages could reduce the accumulation of foam cells, and inhibit the formation and development of plaque. Our results showed autophagy-null macrophages exhibited defective cholesterol clearance, impaired efferocytosis, and increased pro-inflammatory phenotype. It suggested that autophagy serves a protective function in M2 macrophages. In the middle and late of AS, autophagy of macrophages can effectively reduce inflammatory response in plaques, and play a role in stabilizing plaques. However, whether when the level of autophagy increases excessively, the fibrous cap can become unstable due to being too thinner is not clear. Some results demonstrated that rapamycin increased expression of M1 markers by promote autophagy [40], while other studies showed that overexpression of TFEB could upregulate autophagy and the expression of pro-inflammatory cytokines remarkably [41].

Our results revealed that the polarization of macrophages from M1 towards M2 phenotype was correlated with the dynamics of atherosclerotic plaque regression. A large number of M2 cells were activated by TNA and increased the production of anti-inflammatory cytokines to play a role in repairing and remodeling damaged tissue effectively. Meanwhile, our results suggested that autophagy induced by TNA served a protective function in cholesterol clearance, repairing efferocytosis and promoting the M2 phenotype. The M2 activation could effectively weaken the inflammatory response due to the polarization of M1; meanwhile, macrophages autophagy could reduce the accumulation of foamy cells and reduce inflammatory response in plaques effectively, and play a role in stabilizing plaques.

MCPIP, a zinc-finger protein, was first identified as a protein induced by MCP-1 in human peripheral blood monocytes [42]. MCP-1 could interact with its receptor CCR2 to cause signal transduction events and result in the induction of MCPIP. Except MCP-1, MCPIP could also be induced by IL-Iβ, TNF-α and IL-6 [43] and some other inflammatory signals. It was reported MCPIP could mediate the production of ROS that cause ER stress and lead to autophagy, and it could inhibit NF-κB activation and contribute to IL-4-induced M2 polarization [44,45].

Krüppel-like factor 4 (KLF4), an evolutionarily conserved zinc finger-containing transcription factor, was considered to cooperate with Stat6 to induce M2 polarization, whereas inhibit M1 polarization via suppressing NF-κB activation [32]. KLF4 can bind the promoter encoding gene of MCPIP. KLF4 and STAT6 cooperatively mediate M2 polarization by upregulating the expression of MCPIP and inhibit M1 polarization via NF-κB by inducing autophagy required for M2 polarization sequentially. Inhibition of KLF4 could attenuate autophagy and M2 polarization, while enhanced M1 polarization accordingly. It is speculated regulating certain key targets such as KLF4 can effectively

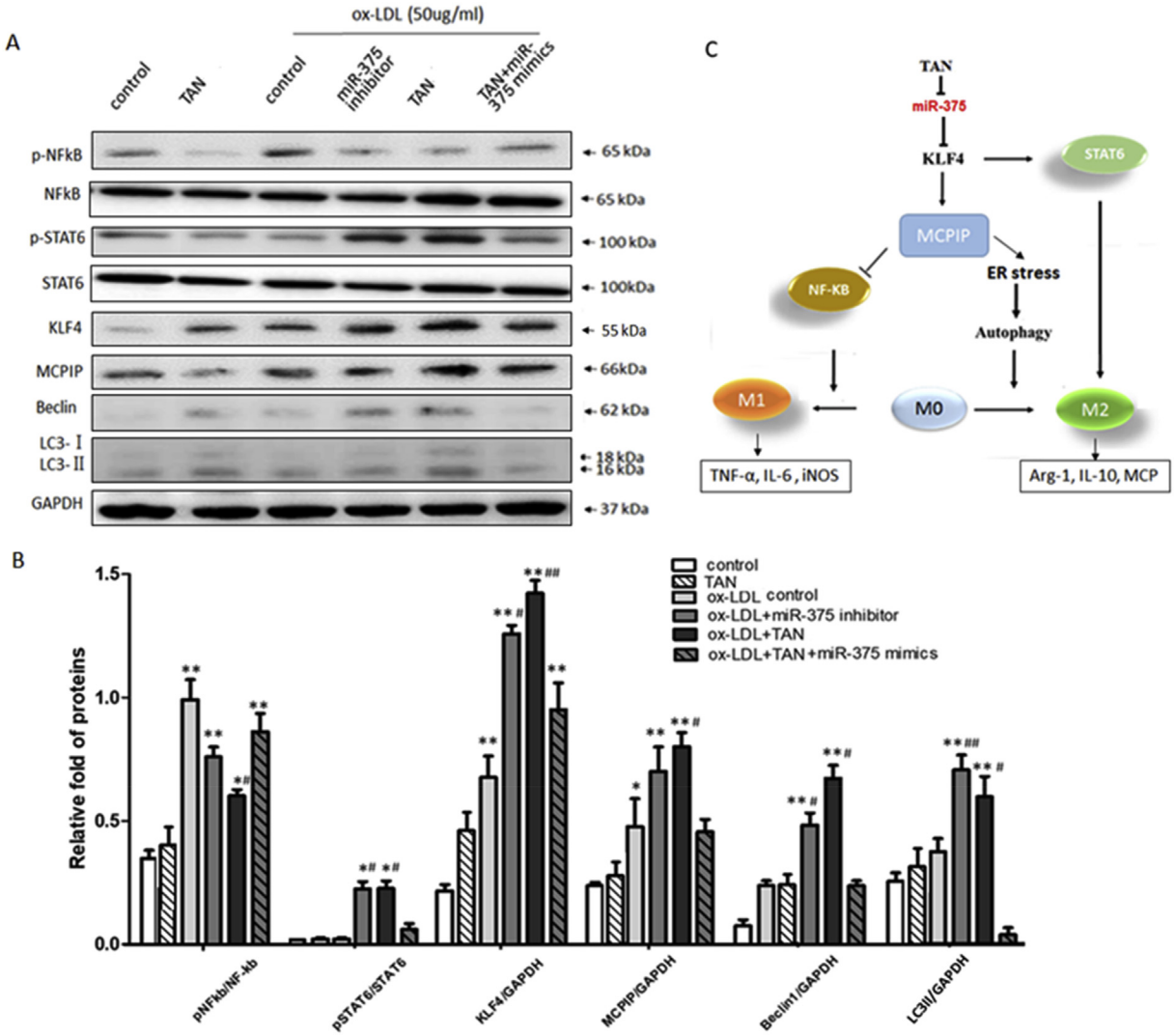

Fig. 5. The analysis of protein levels related to polarization and autophagy signal pathway in RAW264.7 cells treated with ox-LDL and TNA + miR-375 mimics/inhibitor by western blot.

A. The expression of protein in the signaling pathway related with autophagy and polarization of macrophages by western blot. B. The histogram of three independent western blot experiments with statistic results were presented by mean ± SD. n = 3. C. The network of signal pathway of TNA mediates the crosstalk of polarization and autophagy of macrophages. Scheme showing how TNA regulates KLF4 mediates M2 polarization by inhibiting miR-375 and inhibits M1 polarization via NF-κB by sequentially inducing autophagy.

balance activation levels of M1 and M2 macrophages at different stages of AS, and induce moderate autophagy, and improve the stability of AS plaques.

Through the above discussion, we can draw a conclusion that the polarization and autophagy of M1 and M2 macrophages are distinct to induce opposite function and cellular metabolism in atherosclerotic plaques. Whereas both could be modulated by special signal pathway respectively, such as KLF4, STAT6, NF-κB. The crosstalk of this pathway can enhance autophagy of M2 macrophage to promote the decomposition of ox-LDL to liberate free fatty acids (FFA) and cholesterol efflux. While in M1 macrophages, it can induce a defective autophagy, which is associated with hyperactivation of inflammasome, increasement of IL-6, and formation of cholesterol crystals. Autophagy is important for an efficient efferocytosis in apoptotic plaque macrophages. Therefore, autophagy is believed to be a significant process in the reparative M2 macrophage phenotype in the process of forming atherosclerotic plaques, and defective autophagy in macrophages may lead to the less beneficial M1 phenotypic change.

The results suggested TNA could induced macrophages in atherosclerotic plaque to M2 type through p-STAT6 pathway and express moderate levels of autophagy; while attenuate polarization of M1 type through downregulating p-NF-κB pathway. It was shown that miR-375/KLF4 pathway played a dominant role in macrophages polarization as well as autophagy. It was suggested the activation of KLF4 through inhibiting miR-375 by TNA could enhance autophagy and upregulate the producing of anti-inflammatory cytokines, such as arginase-1, IL-10 and MCP, and inhibition of the secretion of pro-inflammatory cytokines, such as TNF-α, IL-6 and iNOS, then resulted in M2 polarization. The signaling pathway was portrayed in Fig. 5C.

It is believed that the basic or moderate autophagy is an important protection against oxidative stress and inflammation in AS plaque, and a necessary determinant for AS plaque stability. It is speculated regulating certain key targets (such as KLF4, mTOR, PI3K, etc.) can effectively balance activation levels of M1 and M2 macrophages at different stages of AS, and induce moderate autophagy, improve the stability of AS plaques.

In summary, this study explored the internal immune mechanism of TNA mediating the crosstalk of polarization and autophagy in macrophages, and elucidated the exact mechanism of TNA in treatment for atherosclerosis through anti-miR-375 therapy to reduce inflammatory

response. Taken together, our studies might provide the basis for further revealing pathogenesis of AS and find out more effective drug for the therapy of arteriosclerosis and other CVDs.

List of support/grant information

1. National Natural Science Foundation of China grant (No. 81300229, 81874372)
2. The open fund from Key Laboratory of Ministry of Education for TCM Viscera-State Theory and Applications (ZYZX1602), Liaoning University of Traditional Chinese Medicine, China.
3. Key Basic Research Project of Liaoning Ministry of Education (L201701).

Conflict of interest

We declare that the authors do not have any competitive interest that might affect the outcome and/or discussion of this paper.

Funding

This work was financially supported by National Natural Science Foundation of China grant (No. 81300229 and 81874372 to Wenna Chen); Key Basic Research Project of Liaoning Ministry of Education (L201701) to Wenna Chen); the open fund from Key Laboratory of Ministry of Education for TCM Viscera-State Theory and Applications (ZYZX1602), Liaoning University of Traditional Chinese Medicine, and Young and Middle-aged Science and Technology Innovation Talent Support Plan of Shenyang, China (RC180069).

Author contributions

Wenna Chen performed the majority of experiments, and wrote the paper; Junyan Wang and Nan Song contributed to the generation of ApoE$^{-/-}$ mice; Lianqun Jia provided assistance in experimental design; Shengnan Guo performed ELISA, WB and qPCR; Ximing Li participated in the experiment design and reviewed the paper.

Acknowledgment

We are grateful for the assistance from Hongwei Sun and Xiande Ma in animal studies.

Appendix A. Supplementary data

Supplementary data to this article can be found online at https://doi.org/10.1016/j.intimp.2019.02.054.

References

[1] M. Benoit, B. Desnues, J.L. Mege, Macrophage polarization in bacterial infections, J. Immunol. 181 (2008) 3733–3739.
[2] Chen W, Liu J, Meng J, Lu C, Li X, et al. Macrophage polarization induced by neuropeptide methionine enkephalin (MENK) promotes tumoricidal responses. Cancer Immunol. Immunother.. 61 (2012) 1755–1768.
[3] Bouhlel MA, Derudas B, Rigamonti E, Dièvart R, Brozek J, et al. PPARg activation primes human monocytes into alternative M2 macrophages with anti-inflammatory properties. Cell Metab.. 6 (2007)137–143.
[4] S. Gordon, F.O. Martinez, Alternative activation of macrophages: mechanism and functions, Immunity 32 (2010) 593–604.
[5] Kadl A, Meher AK, Sharma PR, Lee MY, Doran AC, et al. Identification of a novel macrophage phenotype that develops in response to atherogenic phospholipids via Nrf2. Circ. Res.. 107 (2010) 737–746.
[6] C.A. Gleissner, I. Shaked, K.M. Little, K. Ley, CXC chemokine ligand 4 induces a unique transcriptome in monocyte-derived macrophages, J. Immunol. 184 (2010) 4810–4818.
[7] Chistiakov DA, Bobryshev YV, Nikiforov NG, Elizova NV, Sobenin IA, et al. Macrophage phenotypic plasticity in atherosclerosis: the associated features and the peculiarities of the expression of inflammatory genes. Int. J. Cardiol. 1 (2015) 436–45.
[8] B.G. Hill, P. Haberzettl, Y. Ahmed, S. Srivastava, A. Bhatnagar, Unsaturated lipid peroxidation-derived aldehydes activate autophagy in vascular smooth-muscle cells, Biochem. J. 410 (2008) 525–534.
[9] Karantza-Wadsworth V, Patel S, Kravchuk O, Chen G, Mathew R, et al. Autophagy mitigates metabolic stress and genome damage in mammary tumorigenesis. Genes Dev.. 21 (2007)1621–1635.
[10] T. Yorimitsu, U. Nair, Z. Yang, D.J. Klionsky, Endoplasmic reticulum stress triggers autophagy, J. Biol. Chem. 281 (2006) 30299–30304.
[11] J. Huang, G.Y. Lam, J.H. Brumell, Autophagy signaling through reactive oxygen species, Antioxid. Redox Signal. 14 (2011) 2215–2231.
[12] Matsuzawa T, Kim BH, Shenoy AR, Kamitani S, Miyake M, et al. IFN-gamma elicits macrophage autophagy via the p38 MAPK signaling pathway. J. Immunol.. 189 (2012) 813–818.
[13] Razani B, Feng C, Coleman T, Emanuel R, Wen H, et al. Autophagy links inflammasomes to atherosclerotic progression. Cell Metab.. 15 (2012) 534–544.
[14] Ouimet, M., Franklin, V., Mak, E., Liao, X., Tabas, I., et al. Autophagy regulates cholesterol efflux from macrophage foam cells via lysosomal acid lipase. Cell Metab.. 13 (2011) 655–667.
[15] M. Ouimet, Autophagy in obesity and atherosclerosis: interrelationships between cholesterol homeostasis, lipoprotein metabolism and autophagy in macrophages and other systems, Biochim. Biophys. Acta 1831 (2013) 1124–1133.
[16] B.J. McEwen, The influence of herbal medicine on platelet function and coagulation: a narrative review, Semin. Thromb. Hemost. 41 (2015) 300–314.
[17] Gao S, Liu Z, Li H., Little PJ, Liu P, et al. Cardiovascular actions and therapeutic potential of tanshinone IIA. Atherosclerosis 220 (2012) 3–10.
[18] F. Maione, N. Mascolo, Danshen and the cardiovascular system: new advances for an old remedy, Semin. Thromb. Hemost. 42 (2016) 321–322.
[19] X.H. Tian, J.H. Wu, Tanshinone derivatives: a patent review (January 2006–September 2012), Expert Opin. Ther. Pat. 23 (2013) 19–29.
[20] Y. Zhang, P. Jiang, M. Ye, S.H. Kim, C. Jiang, Tanshinones: sources, pharmacokinetics and anticancer activities, Int. J. Mol. Sci. 13 (2012) 13621–13666.
[21] Maione F, Cantone V, Chini MG, De Feo V, Mascolo N, et al. Molecular Mechanism of Tanshinone IIA and Cryptotanshinone in Platelet Anti-aggregating Effects: An Integrated Study of Pharmacology and Computational Analysis vol. 100 (2015) 174–178.
[22] Yang JX, Pan YY, Ge JH, Chen B, Mao W, et al. Tanshinone II A attenuates TNF-α-induced expression of VCAM-1 and ICAM-1 in endothelial progenitor cells by blocking activation of NF-κB. Cell. Physiol. Biochem. 40 (2016) 195–206.
[23] Garikipati VNS, Verma SK, Jolardarashi D, Cheng Z, Ibetti J, et al. Therapeutic inhibition of mi R-375 attenuates post-myocardial infarction inflammatory response and left ventricular dysfunction via PDK-1-AKT signalling axis Cardiovasc. Res.. 113 (2017) 938–949.
[24] Ke QH, Chen HY, He ZL, Lv Z, Xu XF, et al. Silencing of microRNA-375 affects immune function in mice with liver failure by upregulating astrocyte elevated gene-1 through reducing apoptosis of Kupffer cells J. Cell. Biochem.. 120 (2019) 253–263.
[25] Zirlik A, Maier C, Gerdes N, MacFarlane L, Soosairajah J, et al. CD40 ligand mediates inflammation independently of CD40 by interaction with mac-1. Circulation. 115 (2007) 1571–1580.
[26] Ai D, Jiang H, Westerterp M, Murphy AJ, Wang M, et al. Disruption of mammalian target of rapamycin complex 1 in macrophages decreases chemokine gene expression and atherosclerosis, Circ. Res. 114 (2014) 1576–1584.
[27] Maiseyeu A, Badgeley MA, Kampfrath T, Mihai G, Deiuliis JA, et al., In vivo targeting of inflammation-associated myeloid-related protein 8/14 via gadolinium immunonanoparticles. Arterioscler. Thromb. Vasc. Biol.. 32 (2012) 962–70.
[28] D.B. Munafo, M.I. Colombo, A novel assay to study autophagy: regulation of autophagosome vacuole size by amino acid deprivation, J. Cell Sci. 114 (2001) 3619–3629.
[29] Nidhi Kapoor, Jianli Niu, Yasser Saad, Sanjay Kumar, Tatiana Sirakova, et al. Transcription factors STAT6 and KLF4 implement macrophage polarization via the dual catalytic powers of MCPIP, J. Immunol.. 194 (2015) 6011–6023.
[30] T. Lawrence, G. Natoli, Transcriptional regulation of macrophage polarization: enabling diversity with identity, Nat. Rev. Immunol. 11 (2011) 750–761.
[31] A. Sica, A. Mantovani, Macrophage plasticity and polarization: in vivo veritas, J. Clin. Invest. 122 (2012) 787–795.
[32] Liao X, Sharma N, Kapadia F, Zhou G, Lu Y, et al. Krüppel-like factor 4 regulates macrophage polarization. J. Clin. Invest. 121 (2011) 2736–2749.
[33] Khallou-Laschet J, Varthaman A, Fornasa G, Compain C, Gaston AT, et al. Macrophage plasticity in experimental atherosclerosis. PLoS One. 5 (2010) e8852.
[34] Lefèvre L, Galès A, Olagnier D, Bernad J, Perez L, et al. PPAR gamma ligands switched high fat diet-induced macrophage M2b polarization toward M2a thereby improving intestinal Candida elimination. PLoS One. 5 (2010) e12828.
[35] G.J. Randolph, Mechanisms that regulate macrophage burden in atherosclerosis, Circ. Res. 114 (2014) 1757–1771.
[36] Stöger JL, Gijbels MJ, van der Velden S, Manca M, van der Loos CM, et al. Distribution of macrophage polarization markers in human atherosclerosis. Atherosclerosis. 225 (2012) 461–8.
[37] Chinetti-Gbaguidi G, Baron M, Bouhlel MA, Vanhoutte J, Copin C, et al. Human atherosclerotic plaque alternative macrophages display low cholesterol handling but high phagocytosis because of distinct activities of the PPAR gamma and LXR alpha pathways. Circ. Res.. 108 (2011) 985–95.
[38] Brochériou I, Maouche S, Durand H, Braunersreuther V, Le Naour G, et al. Antagonistic regulation of macrophage phenotype by M-CSF and GM-CSF: implication in atherosclerosis. Atherosclerosis. 214 (2011) 316 – 324.
[39] Van Tits LJ, Stienstra R, van Lent PL, Netea MG, Joosten LA, et al. Oxidized LDL enhances pro-inflammatory responses of alternatively activated M2 macrophages: a

crucial role for Kruppel-like factor 2. Atherosclerosis. 214 (2011) 345 – 349.
[40] Chen W, Ma T, Shen XN, Xia XF, Xu GD, et al. Macrophage-induced tumor angiogenesis is regulated by the TSC2-mTOR pathway. Cancer Res.. 72 (2012) 1363–1372.
[41] Visvikis O, Ihuegbu N, Labed SA, Luhachack LG, Alves AM, et al. Innate host defense requires TFEB-mediated transcription of cytoprotective and antimicrobial genes. Immunity. 40 (2014) 869–909.
[42] Zhou L, Azfer A, Niu J, Graham S, Choudhury M, et al. Monocyte chemoattractant protein-1 induces a novel transcription factor that causes cardiac myocyte apoptosis and ventricular dysfunction. Circ. Res. 98 (2006) 1177–1185.
[43] Liang J, Wang J, Azfer A, Song W, Tromp G, et al. A novel CCCH-zinc finger protein family regulates proinflammatory activation of macrophages. J. Biol. Chem. 283 (2008) 6337–6346.
[44] Liang J, Saad Y, Lei T, Wang J, Qi D, et al. MCP-induced protein 1 deubiquitinates TRAF proteins and negatively regulates JNK and NF-kappaB signaling. J. Exp. Med. 207 (2010) 2959–2973.
[45] C.W. Younce, P.E. Kolattukudy, MCP-1 causes cardiomyoblast death via autophagy resulting from ER stress caused by oxidative stress generated by inducing a novel zinc-finger protein, MCPIP, Biochem. J. 426 (2010) 43–53.